

REVIEW ARTICLE

Principles and Clinical Application of Dual-energy Computed Tomography in the Evaluation of Cerebrovascular Disease

Charlie Chia-Tsong Hsu, Gigi Nga Chi Kwan, Dalveer Singh, Jit Pratap, Trevor William Watkins

Department of Medical Imaging, Princess Alexandra Hospital, Brisbane, Queensland, Australia

Address for correspondence:

Dr. Charlie Chia-Tsong Hsu,
 Department of Medical Imaging,
 Princess Alexandra Hospital, Brisbane,
 Queensland, Australia.
 E-mail: charlie.ct.hsu@gmail.com

"This review article has been previously presented as a poster at the European Congress of Radiology 2016: Hsu CC, Singh D, Kwan GN, Pratap J (2016). Principles and Clinical Application of Dual-Energy CT in the Evaluation of Cerebrovascular Disease. doi: 10.1594/ecr2016/C-0811."



Received : 31-03-2016
 Accepted : 23-05-2016
 Published : 29-06-2016

ABSTRACT

Dual-energy computed tomography (DECT) simultaneously acquires images at two X-ray energy levels, at both high- and low-peak voltages (kVp). The material attenuation difference obtained from the two X-ray energies can be processed by software to analyze material decomposition and to create additional image datasets, namely, virtual noncontrast, virtual contrast also known as iodine overlay, and bone/calcium subtraction images. DECT has a vast array of clinical applications in imaging cerebrovascular diseases, which includes: (1) Identification of active extravasation of iodinated contrast in various types of intracranial hemorrhage; (2) differentiation between hemorrhagic transformation and iodine staining in acute ischemic stroke following diagnostic and/or therapeutic catheter angiography; (3) identification of culprit lesions in intra-axial hemorrhage; (4) calcium subtraction from atheromatous plaque for the assessment of plaque morphology and improved quantification of luminal stenosis; (5) bone subtraction to improve the depiction of vascular anatomy with more clarity, especially at the skull base; (6) metal artifact reduction utilizing virtual monoenergetic reconstructions for improved luminal assessment postaneurysm coiling or clipping. We discuss the physical principles of DECT and review the clinical applications of DECT for the evaluation of cerebrovascular diseases.

Key words: Artifacts, atherosclerotic, carotid stenosis, cerebrovascular disorders, intracranial hemorrhages, multidetector computed tomography, plaque

INTRODUCTION

The concept of dual-energy computed tomography (DECT) is based on the attenuation differential of various materials when simultaneously exposed to low- and high-energy

X-rays.^[1] This reflects the difference in material interaction with low- and high-energy photons and resultant changes in Compton scatter and photoelectric effects.^[1,2] Compton scatter (scattering of X-rays with little absorption) predominates at

This is an open access article distributed under the terms of the Creative Commons Attribution-NonCommercial-ShareAlike 3.0 License, which allows others to remix, tweak, and build upon the work non-commercially, as long as the author is credited and the new creations are licensed under the identical terms.

For reprints contact: reprints@medknow.com

How to cite this article: Hsu CC, Kwan GN, Singh D, Pratap J, Watkins TW. Principles and Clinical Application of Dual-energy Computed Tomography in the Evaluation of Cerebrovascular Disease. J Clin Imaging Sci 2016;6:27.
 Available FREE in open access from: <http://www.clinicalimagingcience.org/text.asp?2016/6/1/27/185003>

| Access this article online | |
|---|--|
| Quick Response Code: | Website: www.clinicalimagingcience.org |
|  | DOI: 10.4103/2156-7514.185003 |

the 120–140 peak kilovoltage (kVp) energy range.^[2] In contrast, the photoelectric effect (photon absorption) is specific to an element and equates to the energy required to eject a K-shell electron.^[2] The photoelectric effect is proportional to the cube of the atomic number and inversely proportional to the incident photon energy (Z^3/E^3). Conventional CT utilizes a single polychromatic X-ray tube with a peak energy of approximately 120 kVp and produces images with high signal-to noise ratio; however, clear discrimination between different high attenuation materials such as iodine, hematoma and bone, or calcium can sometimes be difficult and may require additional acquisitions such as a noncontrast scan. Currently, two different DECT technologies are in clinical usage. One method employs two orthogonal X-ray tubes set at different kVp levels with two separate detectors.^[1] The second method uses rapid kVp switching from a single X-ray source and a detector composed of two scintillation layers.^[1] In both methods, the two energy levels are typically set at 80–100 kVp and 140 kVp.^[1]

PRINCIPLE OF MATERIAL DECOMPOSITION

DECT principle works on a method of material decomposition. In this method, the attenuation of fundamental materials is discernibly different from one another such as cerebrospinal fluid, brain parenchyma, hematoma, iodine and, calcification. A plot of the behavior of the energy attenuation on both X-ray tubes results in a physiological line reflecting the graduated increase in expected Hounsfield units in each voxel with higher density material.^[1,3,4] Presence of iodine within voxel changes the attenuation profile significantly and results in an upward deviation from the physiological line, and the gradient of the slope corresponds to the iodine concentration within the voxel where higher iodine concentration results in a larger gradient [Figure 1]. This change in attenuation profile is reflective of the binding energy of the K-shell electron (K-edge) of iodine which is 33.2 keV that is closer to the mean energy of the lower energy X-ray tube on a DECT scanner, which is typically set as either 80 kV or 100 kV. This translates to nearly a two-fold increase in the attenuation level of iodine on 80 kV images compared to the 140 kV images.^[1-4] Pathologies, which result in increased iodine concentration from either extravasation and/or neovascularity, will exhibit this unique dual energy property. Complex algorithms have been developed to analyze the DECT data using material decomposition algorithms based on the dual energy properties of material to differentiate brain parenchyma, hemorrhage, and iodine. Standard multiplanar reconstructions are created on the weighted average image (weighting factor of 0.4), which resembles the conventional 120-kVp image of single-energy CT [Figure 2]. In addition, a virtual noncontrast (VNC) image can be created by the

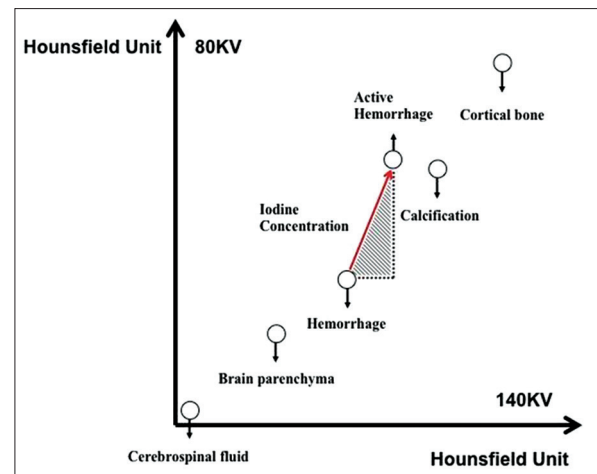


Figure 1: Principle of material decomposition algorithm is based on the different attenuation profiles of brain parenchyma, hematoma, and iodine. Measured voxel values are plotted on the dual-energy scatterplot. Cerebrospinal fluid, brain parenchyma, and hematoma show similar Hounsfield unit value on both 80 and 140 kV images. In contrast, iodine shows a two-fold increase in Hounsfield unit value on 80 kV compared with 140 kV. The gradient of the slope (red arrow) correlate with the iodine concentration and increased gradient reflect greater concentration of iodine.

removal of iodine with no additional radiation exposure, closely mimicking the noncontrast image obtained from single-energy CT. Virtual contrast (VC) image, also known as iodine overlay, can also be generated to enhance depiction of iodine contrast concentration and distribution. When necessary, additional bone and calcium subtraction images can be generated to allow better depiction of vessel lumens that would otherwise be obscured by bone or calcified atheromatous plaque. Virtual monoenergetic images are useful to reduce the artifact surrounding metallic aneurysm coils or clips.

DIFFERENTIATION BETWEEN HEMORRHAGE AND IODINE CONTRAST

The presence of contrast extravasation on CT angiography (CTA) within a parenchymal hemorrhage, also known as the "spot sign", has been shown to be associated with hematoma expansion and correlated with poor prognosis.^[5-8] The accurate depiction of a "spot sign(s)", therefore, potentially serves as a rapid noninvasive biomarker for higher risk hematomas and may directly influence decisions for medical or surgical management.^[9] Currently, four phase II randomized trials are underway to investigate the efficacy of early treatment with either recombinant activated factor VII or tranexamic acid in patients at a high risk for hematoma growth as depicted by the presence of a "spot sign" on CT angiogram (STOP-IT [ClinicalTrials.gov NCT00810888], SPOTLIGHT [ClinicalTrials.gov NCT01359202], TRAIGE [ClinicalTrials.gov NCT02625948], and STOP-AUST [ClinicalTrials.gov NCT01702636]). DECT improves the detection of subtle contrast extravasation

points by increasing the conspicuity of iodine through the construction of a VC image [Figure 3].^[10] This method reduces radiation dose in comparison to conventional dynamic single-energy CT techniques, which relies on separate multiphase acquisitions (noncontrast, arterial, and delayed/washout phases) to accurately depict active contrast extravasation. Similarly, DECTVC imaging can also be applied for the detection of active bleeding in other types of extra-axial hemorrhage.^[11]

The early recognition of hemorrhagic transformation of ischemic stroke is crucial; however, accurate interpretation can be challenging due to residual parenchymal staining from extravasated iodine contrast during preceding diagnostic or

neurointerventional procedures. DECTVC imaging can again overcome this problem by facilitating accurate differentiation of iodinated contrast from hemorrhage with high sensitivity and specificity.^[12] DECT VC images may be acquired from a noncontrast-enhanced CT head or a CT angiogram study, the latter is particularly useful where there is a need to assess vessel recanalization. Iodine staining should be clearly depicted on the VC image but subtracted on the VNC image, and interpretation of both sets of postprocessing images may improve diagnostic confidence [Figure 4].

The presence of acute intracerebral hemorrhage has the potential to mask an underlying lesion such as a neoplasm or metastases. This ability to differentiate

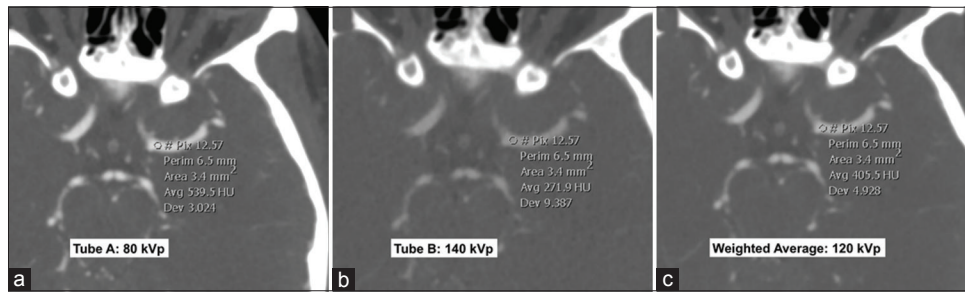


Figure 2: Dual-energy computed tomography angiogram at 80 kVp (a), 140 kVp (b) and weighted average image (c) simulating a 120 kVp image. All the three images displayed are at the same window width and level. Differences in the Hounsfield unit attenuation between the images are illustrated by the Hounsfield unit measurements within the left middle cerebral artery. The lowest energy 80 kVp image (a) shows greatest Hounsfield unit as the energy level is closer to the k-edge of iodine. In contrast, the highest energy 140 kVp image (b) shows lowest Hounsfield unit.

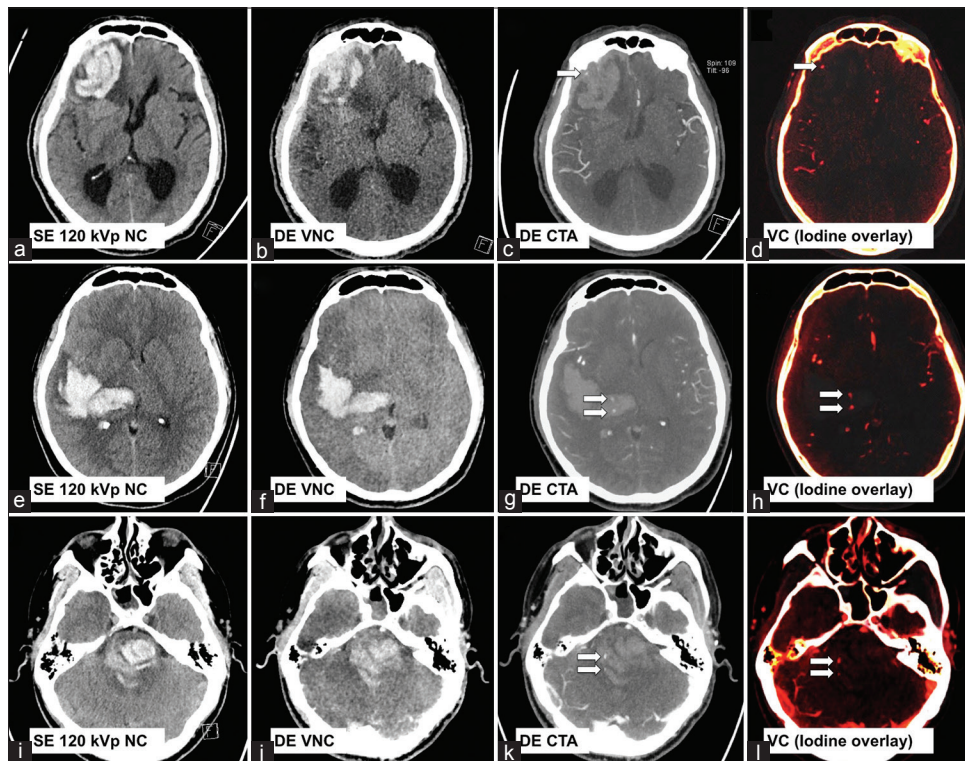


Figure 3: Three examples of cerebral hematoma with active hemorrhage as depicted by a positive “spot sign(s) (arrows) on dual-energy computed tomography angiogram and virtual contrast images. First row: A 78-year-old male with known cerebral amyloid angiopathy (a-d). Second row: A 50-year-old female with poorly controlled hypertension (e-h). Third row: A 26-year-old male with amphetamine abuse (i-l).

between hematoma and iodine may improve the detection of lesions that accumulate iodine contrast due to a pathologic breakdown in blood–brain barrier or tumoral neovascularity. DECT VC image has been shown to be significantly superior to conventional single-energy or weighted average dual energy image for the detection of lesional hemorrhage.^[4] Improved contrast resolution from the VC image is particularly useful in the depiction of focal tumoral enhancement from regional intra- or peri-tumoral hemorrhage [Figure 5].

BONE AND CALCIUM SUBTRACTION

Assessment of head and neck vascular anatomy with CT angiogram or venogram is often obscured by calcified atheromatous plaque or beam hardening artifact at the skull base [Figure 6], which often proves problematic in assessing crucial vessels for pathology. Using material decomposition analysis, DECT postprocessing software allows automated subtraction of osseous or calcified plaques for optimal depiction of the vessel lumen. This technique offers a wide

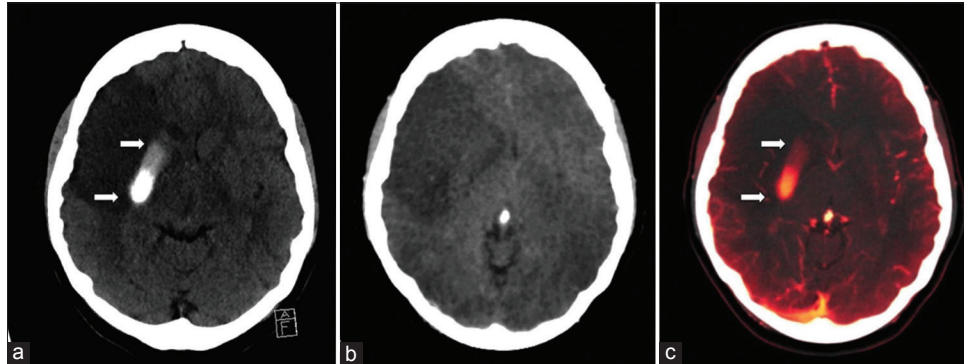


Figure 4: Noncontrast computed tomography of the head (a) shows a focal intraparenchymal hyperdensity in the right lenticular nucleus in a patient following failed clot retrieval for the right middle cerebral artery stroke. Dual-energy computed tomography cerebral angiogram virtual noncontrast image (b) shows subtraction of the right lenticular nucleus hyperdensity (arrows). Virtual contrast image (c) confirms the hyperdensity (arrows) that represents contrast staining. The graduated appearance of the contrast staining may be due to layering/sedimentation.

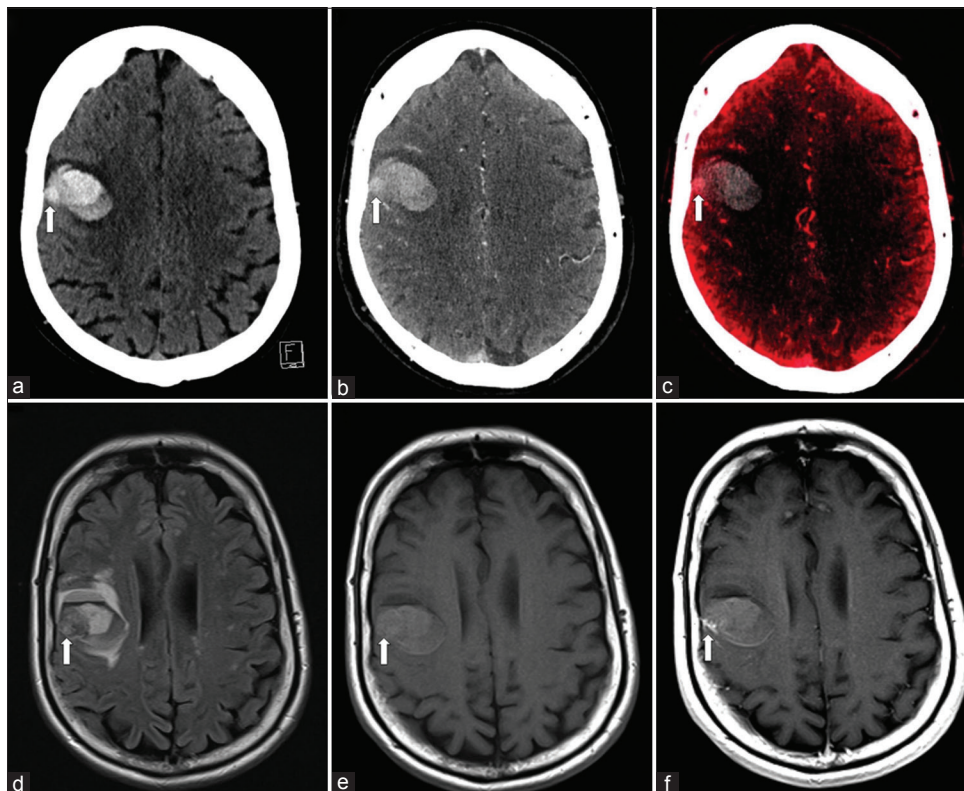


Figure 5: A 50-year-old woman with melanoma metastasis. Single-energy noncontrast computed tomography image (a) shows acute intraparenchymal hemorrhage in the right frontal lobe with a suspicious juxtacortical lesion (arrow) which is difficult to differentiate from surrounding acute hemorrhage. Computed tomography cerebral angiogram (b) again depicts subtle enhancement of the suspected juxtacortical lesion (arrow). Virtual contrast image (c) confirms the presence of a juxtacortical lesion (arrow). Concurrent magnetic resonance imaging brain fluid-attenuated inversion recovery (d), pre- and post-contrast T1-weighted images (e and f) confirms the presence of an enhancing juxtacortical lesion.

range of clinical applications, in particular for the evaluation of carotid plaque morphology and quantification of luminal stenosis.^[3,13-15] DECT can also be used to characterize

the material composition of atheromatous plaques and subtraction of calcium deposits within plaque lesions to improve the assessment of luminal caliber [Figure 7].^[14,15]

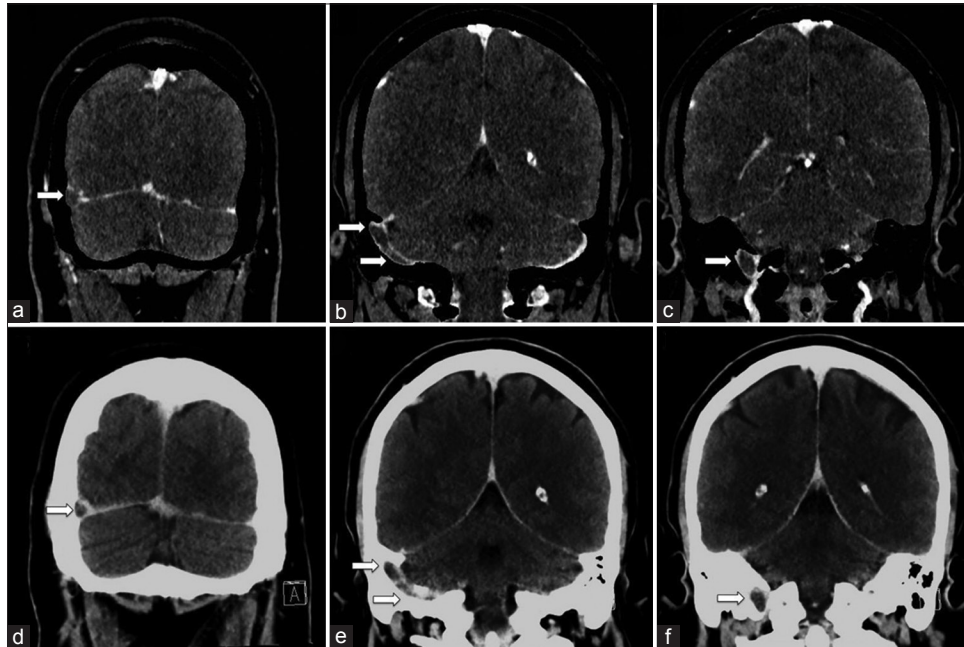


Figure 6: A 38-year-old female with extensive right dural venous sinus thrombosis. Dual-energy computed tomography venogram with bone subtraction images (a-c) shows extensive right dural venous sinus thrombosis involving the distal transverse sinus, sigmoid sinus, and proximal internal jugular vein (arrows). Dual-energy computed tomography venogram without bone subtraction images (d-f) provided for comparison showing the dural venous thrombosis is less conspicuous, especially at the skull base (arrows).

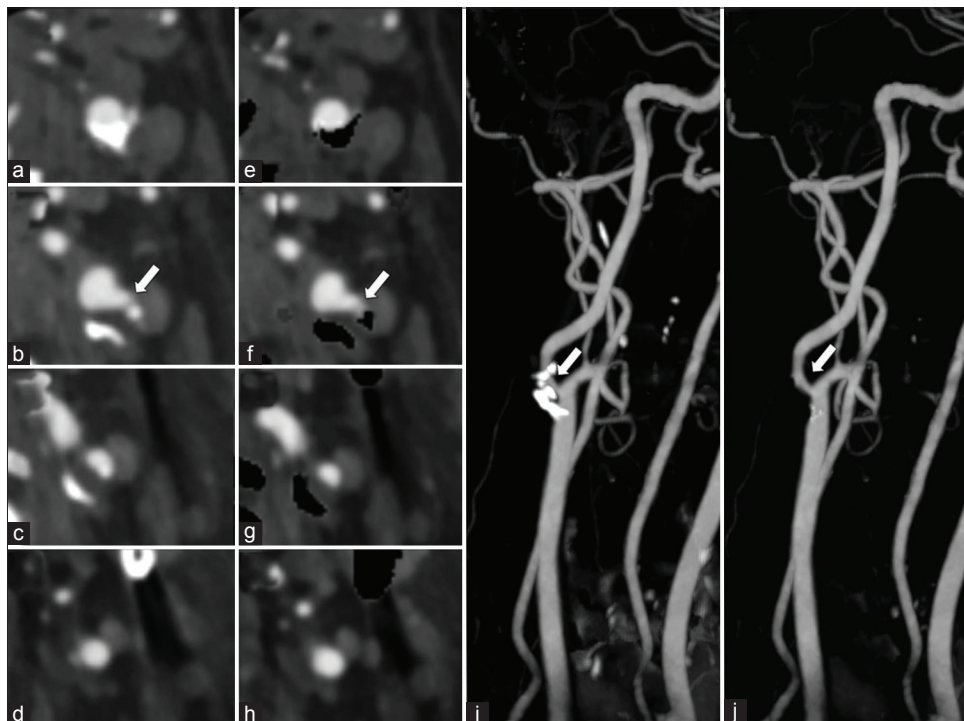


Figure 7: A 60-year-old male with symptomatic left carotid artery stenosis. Dual-energy computed tomography neck angiogram axial images (a-d) and with automatic hard plaque subtraction (e-h) shows moderate-to-high grade stenosis of the right proximal internal carotid artery by hard plaque (arrow). Note the automatic hard plaque subtraction images (e-h) better depict the degree of luminal stenosis than standard axial images (a-d). Rotating maximum intensity projections image (i) and with automatic hard plaque subtraction (j) shows clear visualization of the internal carotid artery which is otherwise obscured by the hard plaque (arrow).

Carotid artery plaque morphology and composition are recognized as important stroke risk factors. Imaging features of the atheromatous plaque that are often considered important in the risk assessment for stroke include the presence of severe stenosis [Figure 8], plaque ulceration, and vasa vasorum enhancement. Subtle plaque ulceration may be obscured from view by adjacent hard calcified plaque, and automated calcium subtraction improves visual assessment [Figure 9]. Although carotid digital subtraction angiography remains the gold standard for the quantification of internal carotid artery stenosis, CTA has become the more popular and accessible imaging modality. Recent data have shown that DECT-automated plaque and bone removal images with maximum intensity projections improve the accuracy of CTA and more closely correlate with digital subtraction angiography compared to standard single-energy CTA.^[16] An interpretation pitfall may be encountered in high grade or critical stenotic lesions when subtracted images can overestimate the severity of stenosis. This can be avoided with careful evaluation of both subtracted and unsubtracted DECT images while correlating with standard reconstructions.^[16]

METAL ARTIFACT REDUCTION

Metal streak artifacts from aneurysm clips or coils greatly degrades image quality and limits accurate assessment

of regional luminal enhancement. Streak artifacts result from both beam hardening and photon starvation, and the severity of the artifact is dependent on the thickness and composition of the metal alloy. Conventional CT techniques have attempted to reduce metallic artifacts by altering gantry angulation, multidetector scanning techniques, iterative reconstruction, and helical scanning with a 3D denoising filter; however, the overall impact on improving image quality has remained minimal.^[1,17-22] Metal artifact reduction on DECT is based on the concept of monochromatic energy. Postprocessing of DECT angiography data allows extraction of the virtual monoenergetic images at the arbitrary photon energies ranging from 30 keV to 130 keV.^[1,23,24] The Hounsfield unit (HU) values within the voxel on the monochromatic energy image reflect the attenuation from a beam of a single energy in contrast to the HU values derived from the polychromatic spectrum of a single-energy multidetector CT.^[1,23,24] The imaging processing algorithm is based on material decomposition and the specific mass attenuation of materials. Theoretically, a true monochromatic image should contain no beam hardening artifacts because of the absence of spectral shifts. Virtual monochromatic image, however, may still be hampered by scatter radiation or photon starvation although the noise level is significantly reduced compared with a single-energy multidetector CT

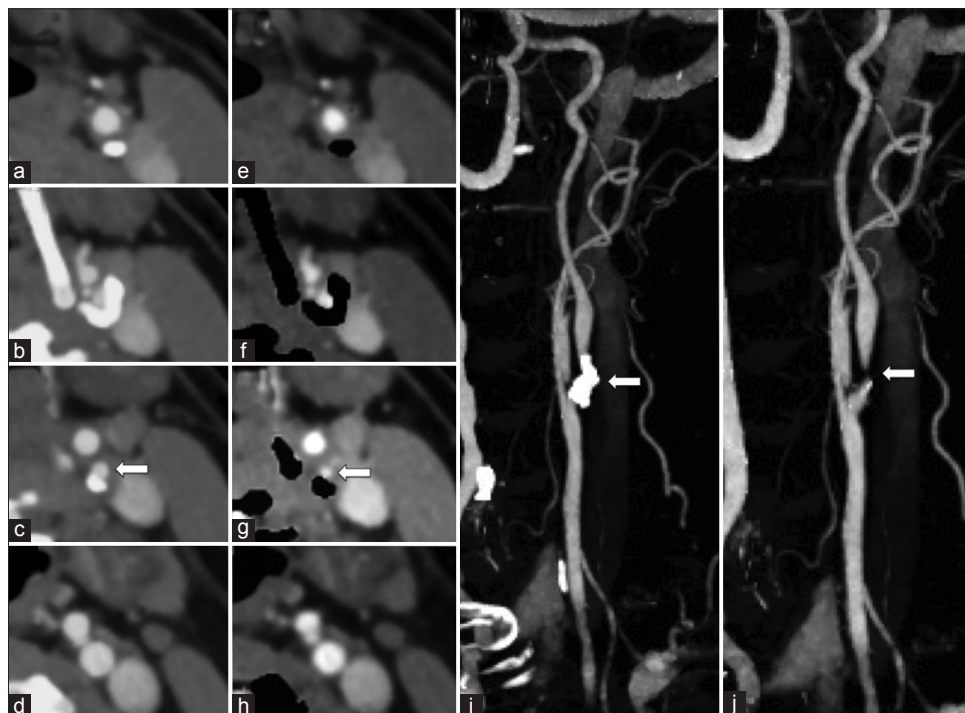


Figure 8: A 67-year-old female with symptomatic left carotid artery stenosis. Dual energy-computed tomography neck angiogram axial images (a-d) and with automatic hard plaque subtraction (e-h) shows high-grade stenosis of the left proximal internal carotid artery by a circumferential hard plaque (arrow). Note the automatic hard plaque subtraction image overestimated the degree of stenosis when compared to the standard axial image. Rotating maximum intensity projections image (i) and with automatic hard plaque subtraction (j) shows the proximal internal carotid artery which is otherwise obscured by the hard plaque (arrow).

polychromatic energy beam.^[1,23] Hence, reducing beam hardening artifacts and providing more quantitatively accurate attenuation measurements are considered to be the main benefits of virtual monoenergetic images. At

lower KeV energy levels, virtual monoenergetic images show greater contrast enhancement of vasculature, but experience a greater degree of beam hardening and scatter effects [Figure 10]. At higher KeV energy levels,

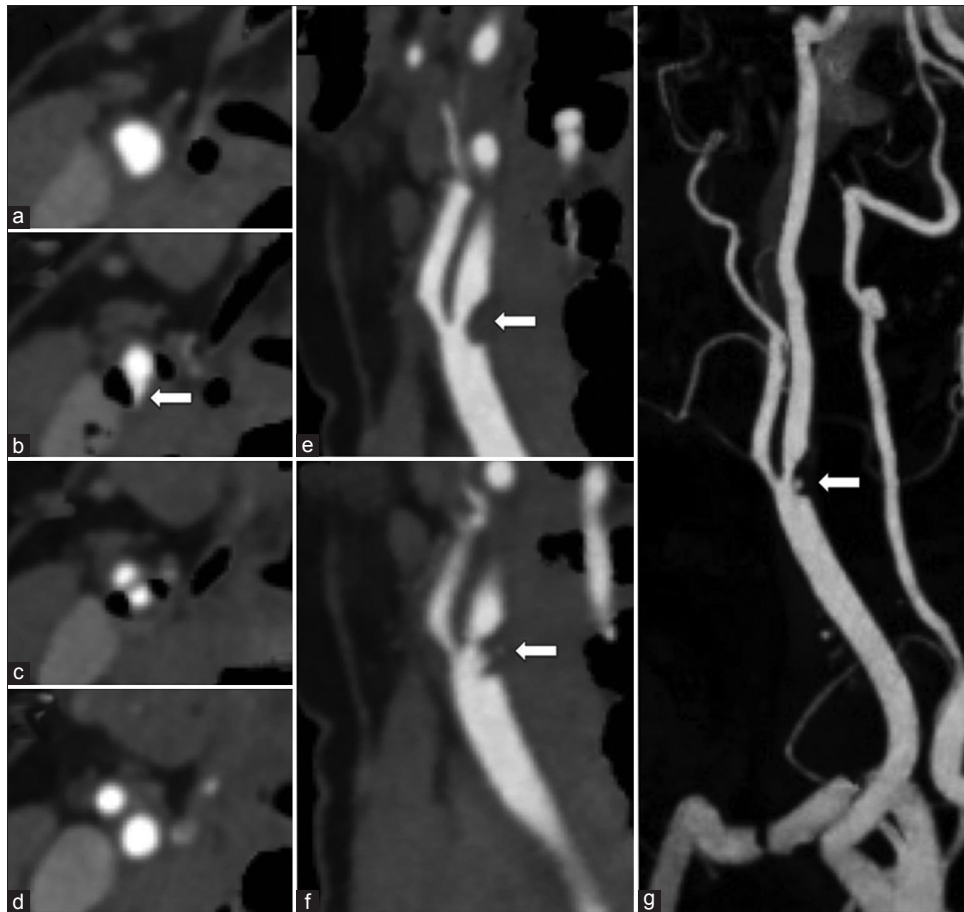


Figure 9: A 38-year-old female with acute right middle cerebral artery ischemic stroke. Dual-energy computed tomography neck angiogram with automatic hard plaque subtraction uncovering a fissured soft plaque flanked by adjacent calcified hard plaque. Axial images (a-d) show mixed morphology plaque at the carotid bifurcation with fissuring of the soft plaque arising from the posterior wall (arrow). Oblique sagittal reformation demonstrates the raised soft plaque from the posterior wall (arrow, e) with an irregular central fissure (arrow, f). Rotation maximum intensity projections with automatic bone and hard plaque subtraction clearly display the fissured soft plaque (arrow, g).

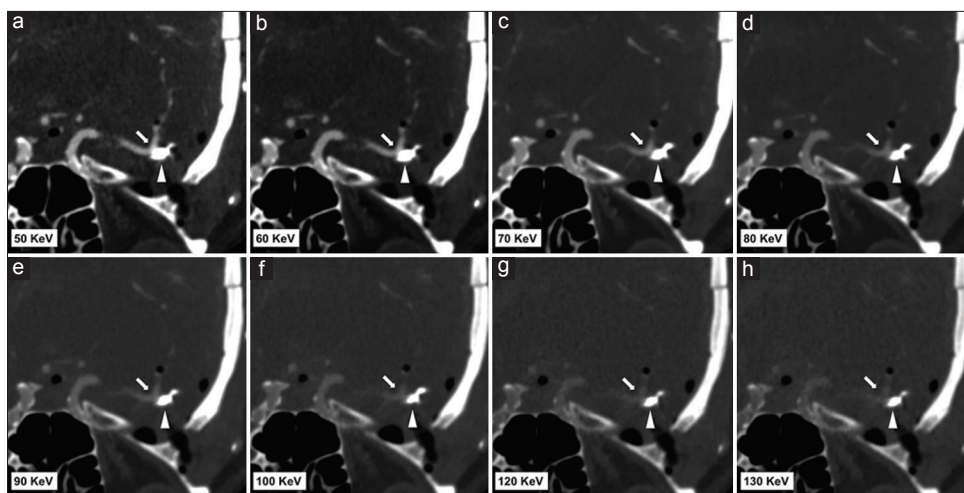


Figure 10: Representative dual-energy computed tomography angiogram images in a 49-year-old female post left middle cerebral artery aneurysm clipping. Images (a-h) are reformatted monoenergetic images at 50 keV, 60 keV, 70 keV, 80 keV, 90 keV, 100 keV, 120 keV, and 130 keV. All images (a-h) set the same window width and level. Beam hardening artifact is reduced at 100–130 keV; however, at higher KeV, the contrast attenuation of the vessel is reduced.

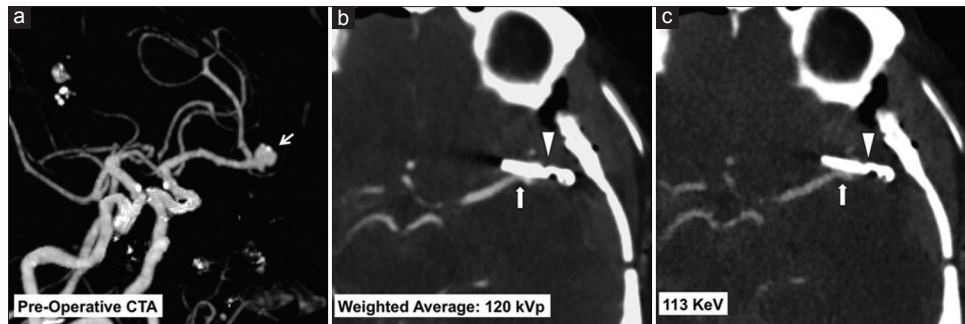


Figure 11: A 49-year-old female with a left middle cerebral artery bifurcation aneurysm treated with clipping. Preoperative dual-energy computed tomography angiogram maximum intensity projections image (a) shows a left middle cerebral artery aneurysm at the M1/M2 junction (arrow). Immediate postoperative dual-energy computed tomography angiogram weighted average 120 kVp image (b) and virtual monoenergetic 113 keV image (c) show the aneurysm clip (arrow head) with improved metal artifact reduction and resolution of the adjacent vessel lumen using the virtual monoenergetic images (arrow, c).

virtual monoenergetic images show a gradual reduction of these artifacts. The trade-off between metal artifact reduction and contrast enhancement implies that optimal virtual monoenergetic images lie within the 90–140 keV range with the median energy level of 113 keV selected as it has the lowest noise value in the area of maximum streak artifact [Figure 11].^[1,25-27] Imaging of aneurysm clips is more notably benefited from the reduced noise level; however, the artifact from aneurysm coiling was less affected by KeV changes.^[25] CTA assessment and surveillance post aneurysm coiling or clipping are set to benefit from this technique, with the alternative imaging modality of magnetic resonance angiogram also frequently hampered by metal blooming artifact limiting detailed luminal assessment.

CONCLUSION

Knowledge of the principles and routine application of DECT in clinical practice is invaluable in problem-solving for a diverse range of cerebrovascular diseases. The postprocessing steps can also be incorporated into certain routine CT protocols to improve diagnostic accuracy, especially in the clinical scenarios of carotid plaque assessments and post-treatment surveillance of cerebral aneurysms. As further DECT techniques emerge from inception and development to implementation in clinical use practice, the role for DECT in neuroimaging can be expected to mature.

Financial support and sponsorship

Nil.

Conflicts of interest

There are no conflicts of interest.

REFERENCES

- Johnson T, Fink C, Schönberg SO, Maximilian FR. Dual Energy CT in Clinical Practice. Heidelberg: Springer; 2011.
- Walter H. Review of Radiological Physics, 3rd ed. Philadelphia, PA: Lippincott Williams and Wilkins; 2003.
- Postma AA, Hofman PA, Stadler AA, van Oostenbrugge RJ, Tijssen MP, Wildberger JE. Dual-energy CT of the brain and intracranial vessels. *AJR Am J Roentgenol* 2012;199 5 Suppl: S26-33.
- Kim SJ, Lim HK, Lee HY, Choi CG, Lee DH, Suh DC, et al. Dual-energy CT in the evaluation of intracerebral hemorrhage of unknown origin: Differentiation between tumor bleeding and pure hemorrhage. *AJNR Am J Neuroradiol* 2012;33:865-72.
- Brouwers HB, Greenberg SM. Hematoma expansion following acute intracerebral hemorrhage. *Cerebrovasc Dis* 2013;35:195-201.
- Huynh TJ, Aviv RI, Dowlatshahi D, Gladstone DJ, Laupacis A, Kiss A, et al. Validation of the 9-point and 24-point hematoma expansion prediction scores and derivation of the PREDICT A/B scores. *Stroke* 2015;46:3105-10.
- Sun SJ, Gao PY, Sui BB, Hou XY, Lin Y, Xue J, et al. “Dynamic spot sign” on CT perfusion source images predicts haematoma expansion in acute intracerebral haemorrhage. *Eur Radiol* 2013;23:1846-54.
- Wada R, Aviv RI, Fox AJ, Sahlas DJ, Gladstone DJ, Tomlinson G, et al. CT angiography “spot sign” predicts hematoma expansion in acute intracerebral hemorrhage. *Stroke* 2007;38:1257-62.
- Steiner T, Bösel J. Options to restrict hematoma expansion after spontaneous intracerebral hemorrhage. *Stroke* 2010;41:402-9.
- Watanabe Y, Tsukabe A, Kunitomi Y, Nishizawa M, Arisawa A, Tanaka H, et al. Dual-energy CT for detection of contrast enhancement or leakage within high-density haematomas in patients with intracranial haemorrhage. *Neuroradiology* 2014;56:291-5.
- Phan CM, Yoo AJ, Hirsch JA, Nogueira RG, Gupta R. Differentiation of hemorrhage from iodinated contrast in different intracranial compartments using dual-energy head CT. *AJNR Am J Neuroradiol* 2012;33:1088-94.
- Gupta R, Phan CM, Leidecker C, Brady TJ, Hirsch JA, Nogueira RG, et al. Evaluation of dual-energy CT for differentiating intracerebral hemorrhage from iodinated contrast material staining. *Radiology* 2010;257:205-11.
- lv P, Lin J, Guo D, Liu H, Tang X, Fu C, et al. Detection of carotid artery stenosis: A comparison between 2 unenhanced MRAs and dual-source CTA. *AJNR Am J Neuroradiol* 2014;35:2360-5.
- Watanabe Y, Nakazawa T, Higashi M, Itoh T, Naito H. Assessment of calcified carotid plaque volume: Comparison of contrast-enhanced dual-energy CT angiography and native single-energy CT. *AJR Am J Roentgenol* 2011;196:W796-9.
- Watanabe Y, Uotani K, Nakazawa T, Higashi M, Yamada N, Hori Y, et al. Dual-energy direct bone removal CT angiography for evaluation of intracranial aneurysm or stenosis: Comparison with conventional digital subtraction angiography. *Eur Radiol* 2009;19:1019-24.
- Thomas C, Korn A, Ketelsen D, Danz S, Tsifikas I, Claussen CD, et al. Automatic lumen segmentation in calcified plaques: Dual-energy CT

- versus standard reconstructions in comparison with digital subtraction angiography. *AJR Am J Roentgenol* 2010;194:1590-5.
17. Jones TR, Kaplan RT, Lane B, Atlas SW, Rubin GD. Single- versus multi-detector row CT of the brain: Quality assessment. *Radiology* 2001;219:750-5.
 18. Kinnunen J, Servo A, Laasonen EM, Porras M. Improved visualization of posterior fossa with clivoaxial CT scanning plane. *Rontgenblatter* 1990;43:539-42.
 19. Sasaki T, Sasaki M, Hanari T, Gakumazawa H, Noshi Y, Okumura M. Improvement in image quality of noncontrast head images in multidetector-row CT by volume helical scanning with a three-dimensional denoising filter. *Radiat Med* 2007;25:368-72.
 20. Schmidt TG. Optimal "image-based" weighting for energy-resolved CT. *Med Phys* 2009;36:3018-27.
 21. Uotani K, Watanabe Y, Higashi M, Nakazawa T, Kono AK, Hori Y, et al. Dual-energy CT head bone and hard plaque removal for quantification of calcified carotid stenosis: Utility and comparison with digital subtraction angiography. *Eur Radiol* 2009;19:2060-5.
 22. Yeoman LJ, Howarth L, Britten A, Cotterill A, Adam EJ. Gantry angulation in brain CT: Dosage implications, effect on posterior fossa artifacts, and current international practice. *Radiology* 1992;184:113-6.
 23. Kuchenbecker S, Faby S, Sawall S, Lell M, Kachelrieß M. Dual energy CT: How well can pseudo-monochromatic imaging reduce metal artifacts? *Med Phys* 2015;42:1023-36.
 24. Tsunoo T, Torikoshi M, Ohno Y, Uesugi K, Yagi N. Measurement of electron density in dual-energy X-ray CT with monochromatic X-rays and evaluation of its accuracy. *Med Phys* 2008;35:4924-32.
 25. Mera D, Santos Armentia E, Bustos A, Villanueva A, Utrera E, Tardaguila FM. Impact of Virtual Monoenergetic Dual-Energy CT on Metal Artifact Reduction After Treatment of Cerebral Aneurysms EPOS Poster Presented at ECR; 2016. doi: 10.1594/ecr2016/C-0246.
 26. Zhou C, Zhao YE, Luo S, Shi H, Li L, Zheng L, et al. Monoenergetic imaging of dual-energy CT reduces artifacts from implanted metal orthopedic devices in patients with fractures. *Acad Radiol* 2011;18:1252-7.
 27. Mera D, Santos Armentia E, Bustos A, Villanueva A, Utrera E, Tardaguila FM. Impact of Virtual Monoenergetic Dual-Energy CT on Metal Artifact Reduction After Treatment of Cerebral Aneurysms EPOS Poster Presented at ECR; 2016. doi: 10.1594/ecr2016/C-0246.